WATER RESOURCES RESEARCH, VOL. 36, NO. 2, PAGES 607–617, FEBRUARY 2000

Slope curvature influence on soil erosion and deposition processes

C. Di Stefano, V. Ferro, P. Porto, and G. Tusa

Sezione Idraulica, Dipartimento di Ingegneria e Tecnologie Agro-Forestali, Università di Palermo, Palermo, Italy

Abstract. Sediment water quality problems are not necessarily the direct result of erosion from the most intense soil erosion areas. A study of within-basin variability of the sediment delivery processes is needed to identify areas where the most effective soil conservation strategies should focus. In this paper the sediment delivery processes is examined along the hydraulic path from sediment source areas to the nearest stream reach. The effects of shape (convex, concave, and uniform) of the hydraulic path are modeled using a power equation for slope profile and revised universal soil loss equation (RUSLE) with two different expressions of the topographic factors. A criterion is proposed for the erosion active slope length, i.e., the slope length in which no deposition processes occur. Then, using the continuity equation for sediment transport, a Ψ factor is deduced to correct the topographic factors of RUSLE and those proposed by *Moore and Burch* [1986], depending on slope curvature. Finally, two relationships for correcting the topographic factors for an irregular slope are experimentally tested comparing the calculated sediment yields with net soil erosion values estimated by the proportional method of *Martz and de Jong* [1987] and cesium 137 data available from a Sicilian basin.

1. Introduction

In recent years, there has been increasing interest in soil conservation practices and cropping systems to keep soil losses at or below tolerable levels. The development of a sustainable agriculture, the estimation of nonpoint pollution [*Novotny and Chesters*, 1989], and the decision processes for land and water resource managers are all problems that need an analytical framework for estimating soil loss and redistribution within a basin.

Recent research has found that the sources of sediment in a stream are not necessarily the areas of most intense soil erosion because of differences in sediment transport capacity. The within-basin variability of the sediment delivery processes [*Walling*, 1983, 1988] has stimulated attempts to model these processes by a spatially distributed approach considering individual fields [*Kling*, 1974; *Julien and Frenette*, 1986, 1987] and the processes of detachment, transport, and deposition [*Nearing et al.*, 1989]. At present the uncertainties of physically based modeling, due to both the equations used to simulate erosion and deposition processes and to the difficulty of measuring or estimating the numerous parameters involved, have favored the development of a parametric approach like revised universal soil loss equation (RUSLE) [*Renard et al.*, 1994] coupled with a spatial disaggregation criterion of sediment delivery processes [*Ferro and Minacapilli*, 1995; *Ferro*, 1997]. The universal soil loss equation (USLE) (and the revised version) is a simple multiplicative model in which four nondimensional factors, representing the influence of topography, crop, and management practices, are used to modify an estimate of basic soil loss called potential erosion. Potential erosion is the product of two parameters representing the influence of rainfall and soil characteristics. The equation was empirically derived and is based on measurements from 2000 plots located in 37 states in the United States. For modeling the within-basin variability of sediment delivery the basin is first divided into morphological units [*Bagarello et al.*, 1993], areas of clearly defined aspect, length, and steepness. Then, using a Lagrangian scheme, sediment particles are followed along their hydraulic path from each morphological unit to the nearest stream reach (Figure 1). Delivery factors are applied to each morphological unit along the hydraulic path. These factors are described below.

Nearly 3 decades of widespread use of the USLE have confirmed its reliability, and it is still considered the best compromise between simplicity of input data and accuracy of soil loss estimate. Despite these statements it is only recently that a study to measure the estimate performance of USLE has been carried out [*Risse et al.*, 1993]. *Risse et al.* [1993] showed that the topographic length-slope (LS) factor and the cover and management factor had the most influence on the model efficiency of the USLE.

Research emphasis has continued to address topographic factors including revised relationships for the LS factors [*McCool et al.*, 1987; *Moore and Wilson*, 1992; *Renard et al.*, 1994] and the slope length exponent of the USLE, which *McCool et al.* [1989] say is affected by slope steepness and the ratio of rill to interrill erosion.

The USLE was primarily designed for, and its standard form has to be applied to, predicting average long-term soil loss on uniform slopes or field units [*Wischmeier and Smith*, 1965, 1978]. Most slopes, however, are not uniform but consist of a sequence of convex, concave, and uniform segments, and the effect of these irregularities on sediment load is not reflected accurately by the overall average steepness [*Foster and Wischmeier*, 1974]. In other words, for a slope with a known slope length and average steepness, erosion varies significantly with slope shape [*Young and Mutchler*, 1969a, b]. According to *Meyer and Kramer* [1969], erosion rate and slope shape interact; the shape of a hillslope affects the rate of erosion at

Paper number 1999WR900157.
0043-1397/00/1999WR900157$09.00

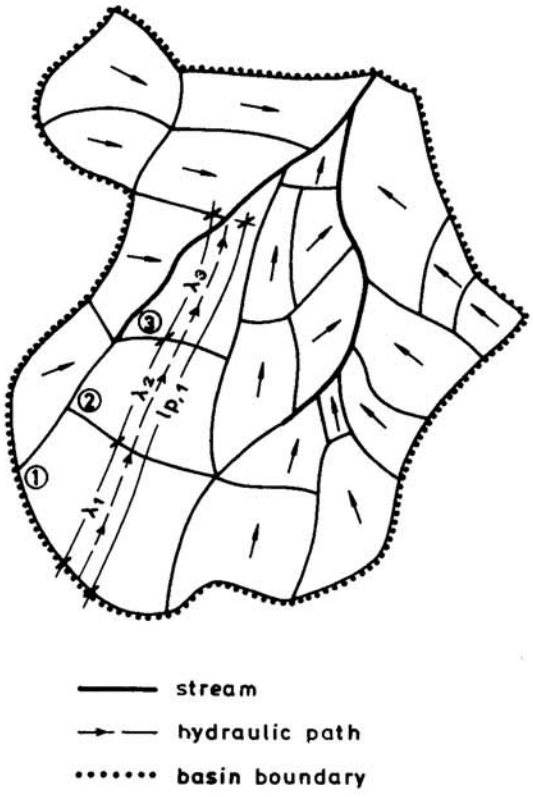

Figure 1. Scheme of the sequential approach.

different locations along the slope, and erosion along a slope changes the slope shape as erosion progresses.

Meyer and Kramer [1969] studied four slope shapes (uniform, convex, concave, and complex, having the upper half convex and lower half concave). The study showed that for the concave and complex slopes most of the upper slope sediment load was deposited along the lower one third of the slope. The analysis also showed that all slope shapes subjected to many erosive events, i.e., considering long-term erosion processes, resemble the concave profile.

Several attempts to adapt the ULSE to irregular slopes have been carried out [*Onstad et al.*, 1967; *Young and Mutchler*, 1969a, b; *Foster and Wischmeier*, 1974; *Castro and Zobeck*, 1986; *Griffin et al.*, 1988]. They generally assumed that net erosion at a particular point on a slope, defined by its distance to the top of slope, is dependent only on conditions at that point.

The USLE applies only to those portions of a slope profile experiencing erosion and not to those areas experiencing deposition. The USLE assumes the process to be detachment limited because sediment load is determined by availability of particles for transport and the sediment load at a given location depends on erosion characteristics of the upslope areas. According to *Foster and Wischmeier* [1974] the erosion process is governed by the following continuity equation for sediment transport:

$$D = \frac{dG}{dx} \tag{1}$$

in which D [t m^{-2} yr^{-1}] is the detachment rate at a point having a distance x from the top of slope and G is the sediment load per unit width. Equation (1) establishes that the quantity of eroded sediment available for transport is equal to the increase of sediment load transported along a slope segment of length dx. Assuming a uniform slope width, G is calculated using USLE [*Wischmeier and Smith*, 1978] to give the following equation:

$$G = \frac{RKCP}{22.1^m} x^{m+1} S(x) \tag{2}$$

in which R is the rainfall erosivity factor [t ha^{-1} per unit of K], K is the soil erodibility factor [t h kg^{-1} m^{-2}], C is the crop and management factor, P is the erosion control practice factor, m is the slope exponent, and S is the slope steepness factor, which has to be written as function of x.

Taking (2) into account and assuming that R, K, C, and P are essentially constant for the entire slope, (1) becomes

$$D = \frac{dG}{dx} = \frac{RKCP}{22.1^m}\left[(m+1)x^m S(x) + x^{m+1}\frac{dS(x)}{dx}\right]. \tag{3}$$

At basin scale the crop factor C is generally characterized by a higher spatial variability than the R, K, and P factors. To establish a simple mathematical function for $C(x)$, which is extremely variable from one basin to the other, we first consider the case $dC/dx = 0$ using an available validating data set in which the crop factor is constant.

Notice that (6) reported by *Foster and Wischmeier* [1974] is obtainable from (3) for $dS(x)/dx = 0$. Equation (6) of *Foster and Wischmeier* [1974] is therefore not a general equation because it assumes that slope steepness is constant. On the contrary, (3) is the general equation describing detachment rate at any location on the land profile. Equation (3) cannot be applied only at those locations where deposition occurs.

For calculating the sediment load G the following integral equation has to be solved:

$$G = \int D\,dx = \frac{RKCP}{22.1^m}\left[\int (m+1)x^m S(x)\,dx + \int x^{m+1}\frac{dS(x)}{dx}\,dx\right]. \tag{4}$$

To complete the integration of (4), an expression of the variable S as function of x is needed. According to *Foster and Wischmeier* [1974] the integration of their (7), which is obtainable from (4) for $dS(x)/dx = 0$, is not simple or practical. They therefore suggest dividing the irregular land profile into segments within which the S factor can be considered constant.

Sediment yield G for the irregular slope can be obtained from the solution of (4) if a mathematical equation to describe the slope profile is adopted. In this paper we first describe the slope steepness s as function of x. Then, using different expressions of the topographic factors [*Wischmeier and Smith*, 1978; *McCool et al.*, 1987; *Moore and Wilson*, 1992; *Renard et al.*, 1994] of (3), we define criterion to identify the erosion active slope length, the length in which deposition processes do not occur. From this we deduce a correction factor for the topographic factors. Finally, we use this relationship to correct the topographic factors for an irregular slope and test it experimentally by comparing calculated sediment yield values with net soil erosion values estimated by measurements of cesium 137 activity and the proportional method of *Martz and de Jong* [1987].

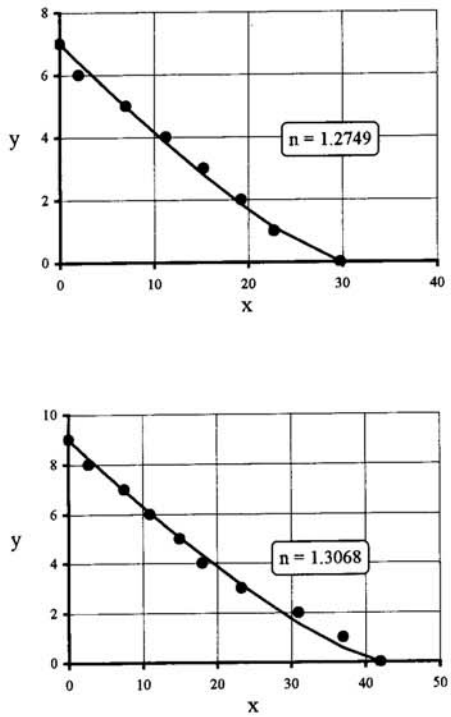

Figure 2. Comparison between the proposed equation of the slope profile and the empirical concave profile.

2. Mathematical Model of Slope Profile and Sediment Delivery

The *Foster and Wischmeier* [1974] approach for calculating the LS factor was also recently extended to two-dimensional terrain, using the concept of the unit contributing area, by *Desmet and Govers* [1996]. Instead of dividing the slope into a number of segments having a constant steepness, (4) can be solved by introducing an equation describing the slope profile.

For describing a topographically complex landscape unit which is characterized by a difference of level H and a slope length λ, which is measured along the horizontal axis, we suggest the following equation:

$$y = H\left(1 - \frac{x}{\lambda}\right)^n \tag{5}$$

in which x is the horizontal abscissa, y is the corresponding elevation, and n is an exponent that varies according to slope shape. The slope length λ is measured along the horizontal axis because this hypothesis will simplify the following mathematical analysis in the range of slope steepness values (2–20%) used in the experimental field tests of *Wischmeier and Smith* [1965]. Equation (5) gives convex profiles for $n < 1$, concave profiles for $n > 1$, and uniform profile for $n = 1$.

The slope steepness s is a function of x and is obtained by differentiation of (5):

$$s(x) = -\frac{dy}{dx} = n\frac{H}{\lambda}\left(1 - \frac{x}{\lambda}\right)^{n-1} = n\frac{H}{\lambda}(1 - x_*)^{n-1} \tag{6}$$

in which x_* is the dimensionless ratio x/λ, with $0 \le x_* \le 1$. Figure 2 shows, as an example, the comparison between the model (equation (5)) and the empirical concave slope profile determined for two hydraulic paths, connecting an upstream morphological unit with the nearest stream reach (Figure 1) in the Sicilian Sparacia basin (Figure 3).

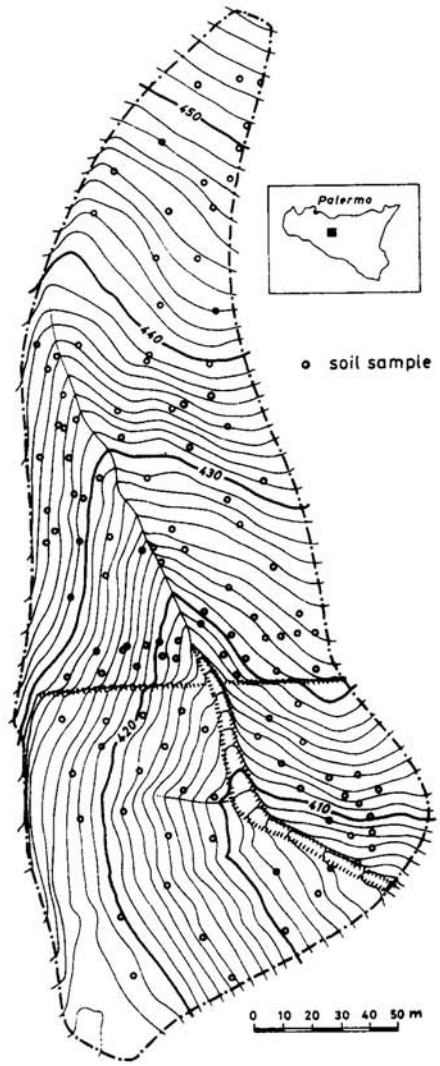

Figure 3. Experimental Sparacia basin.

The concave shape has the most interesting sediment delivery processes at the hillslope scale. In fact, for the concave shape most of the sediment load eroded in the upper part of the slope does not arrive at the channel network because it is deposited in the lower part of the concave profile.

Since sediments are produced from different source areas throughout the basin, the sediment delivery processes would have to be modeled by a spatially distributed approach [*Richards*, 1993]. The physical processes of sediment transport on hillslopes are distinctly different from transport within the channel network. Therefore hillslope sediment delivery processes and channel processes should be considered and modeled separately [*Atkinson*, 1995].

For modeling the hillslope sediment delivery processes the basin is divided into morphological units, considering two effects superimposed: delivery processes occurring along the hydraulic path, from a given morphological unit i and having a

horizontal length $l_{p,i}$ and a mean slope $s_{p,i}$, and deposition due to the concave shape of the hydraulic path profile. The sediment delivery due to the travel time $t_{p,i}$ of each source area, i.e., the time that particles eroded from the source area and transported through the hillslope conveyance system take to arrive at the channel network, decreases both as the length $l_{p,i}$ increases and as the square root of the mean slope $s_{p,i}$ decreases. *Ferro and Minacapilli* [1995] evaluated the travel time of the particles eroded from a given morphological unit i by summing the travel times of all morphological areas along the path between the ith unit and the nearest stream reach (Figure 1). This gives

$$t_{p,i} = \frac{l_{p,i}}{\sqrt{s_{p,i}}} = \sum_{j=1}^{N_p} \frac{\lambda_{i,j}}{\sqrt{s_{i,j}}} \tag{7}$$

in which N_p is the number of morphological units localized along the hydraulic path and $\lambda_{i,j}$ and $s_{i,j}$ are the horizontal length and the mean slope of each of the j morphological areas. *Ferro and Minacapilli* [1995] also proposed to calculate the delivery of eroded sediment particles as the sediment delivery ratio SDR_i of each morphological area. According to *Ferro and Minacapilli*, SDR_i is based on the probability that particles eroded from area i arrive in the nearest stream reach. They gave the following expression [*Ferro and Minacapilli*, 1995; *Ferro*, 1997]:

$$\mathrm{SDR}_i = \exp(-\beta t_{p,i}) \tag{8}$$

in which β is a coefficient, which is assumed to be constant for a given basin [*Ferro et al.*, 1998a, b].

The effect of slope curvature can be taken into account by using, for a concave slope, a modified topographic factor L_cS_c based on the slope profile (equation (5)). According to this scheme the basin is divided into morphological units with hydraulic paths having a quasi-constant slope (uniform hydraulic path) or a concave shape. In the first case the sediment yield Y_i of each morphological unit i is calculated by the following equation:

$$Y_i = R_iK_iL_iS_iC_iP_i\mathrm{SDR}_iS_{u,i} \tag{9}$$

in which R_i is the rainfall erosivity factor of the ith morphological unit, K_i is the soil erodibility factor, L_iS_i is the topographic factor calculated by the horizontal slope length and the mean slope, C_i is the cover and management factor, P_i is the support practice factor, and $S_{u,i}$ is the area of the morphological unit.

The morphological units that define a concave hydraulic path are aggregated as a stream tube for which the sediment yield Y_{st} is calculated according to the following equation:

$$Y_{st} = R_{st}K_{st}L_cS_cC_{st}P_{st}\exp\left(-\beta\frac{l_{st}}{\sqrt{s_{st}}}\right)S_{st} \tag{10}$$

in which R_{st} is the rainfall erosivity factor of the considered stream tube, K_{st} is the soil erodibility factor, C_{st} is the cover and management factor, P_{st} is the support practice factor, l_{st} and s_{st} are the horizontal length and the mean slope of the stream tube, S_{st} is the area of the stream tube, and L_cS_c is the topographic factor, which has to be calculated only for the part of the stream tube profile experiencing erosion. Thus, to apply (10), a criterion is needed for defining the erosion active part or stream tube length in which deposition does not occur.

3. Erosion Active Slope Length and Topographic Factors for Irregular Slopes

According to the RUSLE model [*McCool et al.*, 1989; *Renard et al.*, 1994] the slope factor $S(x)$ of a slope segment of length x and belonging to a slope profile defined by (5) can be calculated by the following relationship:

$$S(x) = a_1s(x) + a_2 = a_1n\frac{H}{\lambda}\left(1 - \frac{x}{\lambda}\right)^{n-1} + a_2 \tag{11}$$

in which a_1 and a_2 are numerical constants having different values for slope steepness, either $<9\%$ ($a_1 = 10.8$ and $a_2 = 0.03$) or greater than or equal to 9% ($a_1 = 16.8$ and $a_2 = -0.5$) [*Moore and Wilson*, 1992]. Equation (11) assumes $\sin\alpha \cong \tan\alpha$, which is reliable for slope angle α values $\leq\pi/6$.

From (11) and the sediment load rate dG/dx, which is expressed by equation (3), it follows that

$$\frac{1}{w}\frac{dG}{dx} = (m+1)x^ma_1n\frac{H}{\lambda}\left(1 - \frac{x}{\lambda}\right)^{n-1} + (m+1)x^ma_2 - x^{m+1}a_1n(n-1)\frac{H}{\lambda^2}\left(1 - \frac{x}{\lambda}\right)^{n-2} \tag{12}$$

in which w is a constant equal to $RKCP/22.1^m$.

Since $x = \lambda x_*$ and $dx = \lambda dx_*$, (12) can be rewritten

$$\frac{1}{w}\frac{dG}{\lambda dx_*} = a_2(m+1)\lambda^m x_*^m + a_1(m+1)nH\lambda^{m-1}x_*^m \cdot (1-x_*)^{n-1} - a_1n(n-1)H\lambda^{m-1}x_*^{m+1} \cdot (1-x_*)^{n-2}$$

and then

$$\frac{dG}{dx_*} = RKCP\left(\frac{\lambda}{22.1}\right)^m\lambda\left[a_2(m+1)x_*^m + a_1 \cdot (m+1)n\frac{H}{\lambda}x_*^m(1-x_*)^{n-1} - a_1n(n-1)\frac{H}{\lambda}x_*^{m+1} \cdot (1-x_*)^{n-2}\right]. \tag{13}$$

The relationship (equation (12)) between

$$\frac{1}{w}\frac{dG}{dx}$$

and the variable x_* for $m = 0.5$ and for fixed values of H, λ, n, a_1, and a_2 is plotted in Figure 4. Figure 4 clearly shows that the variable

$$\frac{1}{w}\frac{dG}{dx}$$

assumes a maximum value for $x_* = x_{*m}$.

Along the active slope profile ($dG/dx > 0$) the detachment rate increases to a maximum value, where there is equality between the actual sediment load and the overland flow transport capacity. Below this point, $D = dG/dx$ decreases ($dG/dx < 0$) because deposition phenomena occur. At x_{*m}, corresponding to the analytical condition

$$\frac{d}{dx}\left(\frac{dG}{dx}\right) = 0$$

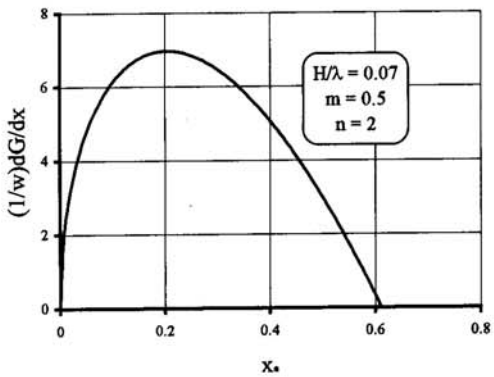

Figure 4. Relationship between the sediment load rate and the dimensionless abscissa x_*.

or

$$\frac{d}{dx_*}\left(\frac{dG}{dx_*}\right) = 0$$

erosion stops because the flow does not detach other particles because transport capacity balances the actual sediment load. This permits defining the erosion active slope length $\lambda_m = \lambda x_{*m}$.

From (13) it follows that x_{*m} is the radix of the following equation:

$$a_2 m(m+1)x_*^{m-1} + a_1 m(m+1)n\frac{H}{\lambda}x_*^{m-1}(1-x_*)^{n-1} - 2a_1(m+1)n(n-1)\frac{H}{\lambda}x_*^{m}(1-x_*)^{n-2} + a_1 n(n-1) \cdot (n-2)\frac{H}{\lambda}x_*^{m+1}(1-x_*)^{n-3} = 0. \quad (14)$$

Equation (14) establishes that the abscissa x_{*m} depends on the mean slope H/λ and the curvature of slope profile represented by the n value. Figure 5 shows the relationship between x_{*m} and n for $m = 0.5$ and for mean slope values ranging from 0.035 to 0.3. Figure 5 also shows that for $m = 0.5$ the relationship $x_{*m} = f(n)$, in which f is a functional symbol, can be represented by the following approximate equation:

$$x_{*m} = \frac{0.820}{n^3} - \frac{0.236}{n^2} + \frac{0.321}{n}. \quad (15)$$

In other words, the relationship $x_{*m} = f(n)$ can be considered independent of the ratio H/λ. For calculating the sediment load $G_{\lambda m}$, transported along the active slope profile length λ_m, (13) has to be integrated for $0 \le x_* \le x_{*m}$:

$$G_{\lambda m} = RKCPL\lambda\left[a_2(m+1)\int_0^{x_{*m}} x_*^m\,dx_* + a_1 n \cdot (m+1)\frac{H}{\lambda}\int_0^{x_{*m}} x_*^m(1-x_*)^{n-1}\,dx_* - a_1 n \cdot (n-1)\frac{H}{\lambda}\int_0^{x_{*m}} x_*^{m+1}(1-x_*)^{n-2}\,dx_*\right]. \quad (16)$$

The integral (16) can be solved taking into account that [*Gradshteyn and Ryzhik*, 1994]

$$\int_0^{x_{*m}} x_*^m\,dx_* = \frac{1}{m+1}x_{*m}^{m+1} \quad (17a)$$

$$\int_0^{x_{*m}} x_*^m(1-x_*)^b\,dx_* = \frac{x_{*m}^{m+1}}{m+1}F(b, m+1, m+2, x_{*m}) \quad (17b)$$

in which $F(b, m+1, m+2, x_{*m})$ is the hypergeometric function having the following definition:

$$F(b, m+1, m+2, x_{*m}) = 1 + \frac{b(m+1)}{(m+2)}x_{*m} + \frac{b(1+b)(m+1)(m+2)}{(m+2)(m+3)2}x_{*m}^2 + \frac{b(1+b)(2+b)(m+1)(m+2)(m+3)}{(m+2)(m+3)(m+4)2\cdot 3}x_{*m}^3 + \cdots. \quad (18)$$

Substituting (17) and (18) into (16), the soil loss $A_{\lambda m}$ (t ha^{-1}) of an active slope 1 m wide can be calculated by the following equation:

$$G_{\lambda m} = \frac{A_{\lambda m}}{\lambda_m} = RKCPL\frac{\lambda}{\lambda_m}\left[a_2 x_{*m}^{m+1} + a_1 n\frac{H}{\lambda}x_{*m}^{m+1}F \cdot (1-n, m+1, m+2, x_{*m}) - a_1 n(n-1) \cdot \frac{H}{\lambda}\frac{x_{*m}^{m+2}}{(m+2)}F(2-n, m+2, m+3, x_{*m})\right]. \quad (19)$$

Equation (19) can be rewritten as

$$A_{\lambda m} = RKCPLS\frac{1}{x_{*m}\left(a_1\dfrac{H}{\lambda} + a_2\right)}\left\{a_1\frac{H}{\lambda}\left[n x_{*m}^{m+1}F \cdot (1-n, m+1, m+2, x_{*m}) - n(n-1)\frac{x_{*m}^{m+2}}{(m+2)}F \cdot (2-n, m+2, m+3, x_{*m})\right] + a_2 x_{*m}^{m+1}\right\}. \quad (20)$$

Therefore (20) assumes the following simple mathematical form:

$$A_{\lambda m} = RKCPLS\Psi(H/\lambda, m, n) \quad (21)$$

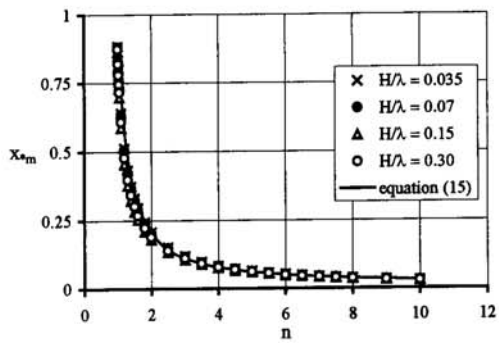

Figure 5. Relationship between x_{*m} and n coefficient.

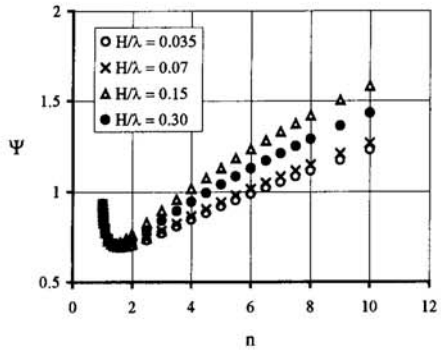

Figure 6. Relationship between Ψ correction factor and n coefficient for revised universal soil loss equation (RUSLE).

in which $\Psi(H/\lambda, m, n)$ is a correction factor for the uniform slope topographic factor having the following expression:

$$\Psi(H/\lambda, m, n) = \frac{1}{\left(a_1 \frac{H}{\lambda} + a_2\right)} \left\{ a_1 \frac{H}{\lambda} \left[n x_{*m}^{m} F(1-n, m+1, m+2, x_{*m}) - \frac{n(n-1)}{(m+2)} x_{*}^{m+1}{}_{m} F(2-n, m+2, m+3, x_{*m}) \right] + a_2 x_{*m}^{m} \right\}. \quad (22)$$

For $m = 0.5$, Figure 6 shows that the relationship $\Psi = f(n)$ can be assumed to be independent of H/λ for $n \leq 1.5$. Figures 5 and 6 show that increasing n (more concave slopes) decreases the erosion active slope length and increases the correction factor value. For a uniform slope length ($n = 1$) that is entirely erosion active ($x_{*m} = 1$), $F(0, m+1, m+2, 1) = 1$, (22) gives $\Psi(H/\lambda, m, 1) = 1$, and (21) assumes the well-known standard form of RUSLE.

The procedure described can also be developed using the topographic factor relationship suggested by *Moore and Burch* [1986] and *Moore and Wilson* [1992]:

$$LS = \left(\frac{cx}{22.1}\right)^{p} \left[\frac{s(x)}{0.0896}\right]^{q} \quad (23)$$

in which c is a shape coefficient [*Bagarello et al.*, 1993] and p and q are numerical constants. Equation (23) is reliable for slopes where $\sin \alpha \cong \tan \alpha$. The sediment load per unit width can be evaluated by the following equation:

$$G = \frac{RKCP}{0.0896^{q}} \left(\frac{c}{22.1}\right)^{p} x^{p+1} s(x)^{q}. \quad (24)$$

The continuity equation for sediment transport gives

$$D = \frac{dG}{dx} = \left[\frac{RKCP}{0.0896^{q}} \left(\frac{c}{22.1}\right)^{p}\right] \left[(p+1) x^{p} s(x)^{q} + x^{p+1} q s(x)^{q-1} \frac{ds(x)}{dx} \right] \quad (25)$$

$$\frac{1}{\varepsilon}\frac{dG}{dx} = (p+1)x^{p}\left[n\frac{H}{\lambda}\left(1-\frac{x}{\lambda}\right)^{n-1}\right]^{q} + qx^{p+1}\left[n\frac{H}{\lambda}\cdot\left(1-\frac{x}{\lambda}\right)^{n-1}\right]^{q-1}\left[-n(n-1)\frac{H}{\lambda^2}\left(1-\frac{x}{\lambda}\right)^{n-2}\right] \quad (26)$$

in which ε is a numerical constant equal to $RKCPc^{p}/0.0896^{q}22.1^{p}$. Introducing the dimensionless variable $x_* = x/\lambda$, (26) can be rewritten as follows:

$$\frac{1}{\varepsilon}\frac{dG}{\lambda dx_*} = (p+1)\frac{n^{q}H^{q}}{\lambda^{q-p}} x_{*}^{p}(1-x_*)^{qn-q} - q \cdot (n-1)\frac{n^{q}H^{q}}{\lambda^{q-p}} x_{*}^{p+1}(1-x_*)^{qn-q-1}$$

and then

$$\frac{1}{\varepsilon}\frac{dG}{\lambda dx_*} = \lambda^{p}\left(\frac{H}{\lambda}\right)^{q}\left[(p+1)n^{q}x_{*}^{p}(1-x_*)^{qn-q} - q \cdot (n-1)n^{q}x_{*}^{p+1}(1-x_*)^{qn-q-1}\right]. \quad (27)$$

From (27) the following relationship is deduced:

$$\frac{dG}{dx_*} = \left[RKCP\left(\frac{c\lambda}{22.1}\right)^{p}\right]\left(\frac{H}{\lambda}\frac{1}{0.0896}\right)^{q} n^{q}\lambda\left[(p+1)x_{*}^{p} \cdot (1-x_*)^{qn-q} - q(n-1)x_{*}^{p+1}(1-x_*)^{qn-q-1}\right]. \quad (28)$$

The function dG/dx_* assumes a maximum value whose abscissa x_{*m} can be determined by (28) by searching the radix of the equation

$$\frac{d}{dx_*}\left(\frac{dG}{dx_*}\right) = 0:$$

$$x_{*}^{p}(1-x_*)^{qn-q}\left[\frac{p(p+1)}{x_*} - \frac{2(p+1)(qn-q)}{(1-x_*)} + q(n-1) \cdot (qn-q-1)\frac{x_*}{(1-x_*)^2}\right] = 0. \quad (29)$$

The abscissa x_{*m} has to be calculated solving the following second-order equation, which is obtained from (29):

$$[p(p+1) + 2(p+1)(qn-q) + (qn-q)(qn-q-1)]x_{*}^{2} - [2p(p+1) + 2(p+1)(qn-q)]x_* + p(p+1) = 0. \quad (30)$$

For $p = 0.6$ and $q = 1.3$, as suggested by *Moore and Wilson* [1992], x_{*m} is the following radix of (30):

$$x_{*m} = \frac{-2.24 + 4.16n - \sqrt{5.82 - 16.64n + 10.82n^2}}{2(-0.21 - 0.52n + 1.69n^2)}. \quad (31)$$

Equation (31) establishes that the abscissa x_{*m} depends, for fixed p and q values, only on the slope curvature.

For calculating the sediment load $G_{\lambda m}$ transported along the active slope profile length λ_m, (28) has to be integrated:

$$G_{\lambda m} = RKCPLS\lambda\left[n^{q}(p+1)\int_{0}^{x_{*m}} x_{*}^{p}(1-x_*)^{qn-q}\,dx_* - n^{q}q(n-1)\int_{0}^{x_{*m}} x_{*}^{p+1}(1-x_*)^{qn-q-1}\,dx_*\right]. \quad (32)$$

Taking (17b) and the definition of the hypergeometric function into account, the soil loss of the active slope can be calculated by (32):

$$A_{\lambda m} = RKCPLS \frac{1}{x_{*m}} \left[n^q x_*^{p+1}{}_m F(q - qn, p + 1, p + 2, x_{*m}) - n^q q(n - 1) \frac{x_*^{p+2}{}_m}{(p + 2)} F(q - qn + 1, p + 2, p + 3, x_{*m}) \right]. \quad (33)$$

Equation (33) also assumes a simple mathematical form like (21):

$$A_{\lambda m} = RKCPLS\Psi(p, q, n) \quad (34)$$

in which the correction factor $\Psi(p, q, n)$ of the uniform slope topographic factor has the following expression:

$$\Psi(p, q, n) = n^q x_{*m}^p F(q - qn, p + 1, p + 2, x_{*m}) - n^q q(n - 1) \frac{x_*^{p+1}{}_m}{p + 2} \cdot F(q - qn + 1, p + 2, p + 3, x_{*m}). \quad (35)$$

Equation (35) establishes that Ψ depends only on p, q, and n because x_{*m}, according to (30), depends only on p, q, and n. Equation (35) can be adequately approximated by the following relationships:

$$\Psi = -6.503n^3 + 26.283n^2 - 35.354n + 16.494 \quad (36a)$$

for $1 < n \leq 1.5$, and

$$\Psi = 0.1229n + 0.4593 \quad (36b)$$

for $n > 1.5$. For $n = 1$, (35) gives $\Psi(p, q, 1) = 1$, and (34) assumes the standard form of RUSLE.

4. Validating the Topographic Factors for Irregular Slopes

4.1. Experimental Methods

We verified the relationships (22) and (35), correcting the topographic factors of RUSLE and *Moore and Burch* [1986], respectively, using cesium 137 measurements carried out in a small Sicilian basin [*Ferro et al.*, 1998b]. Sparacia basin (3.64 ha) is located in the north side of Sicily, Italy (Figure 3). Soil sampling for ^{137}Cs measurements and the soil erodibility factor estimation were carried out at 129 sites uniformly distributed over the basin. A Vertic Xerochrept soil overlays the whole basin; the A horizon is 30 cm deep with a clay texture and a massive/blocky structure.

Taking into account that for clay soils, cesium 137 activity is negligible below a depth of 10 cm, sampling was carried out at each site by coring with two 15 cm long cylinders. From detailed sampling in the upper part of the basin we measured a Cs_{ref} value equal to 94.4 mBq cm^{-2}. We subsampled each of the 129 samples, for particle size distribution, calculating the percentage f of finer particles (particle diameter d ranging from 0.002 to 0.1 mm) and the percentage g of coarser particles ($0.1 < d \leq 2$ mm) according to the procedure of *Wischmeier et al.* [1971]. The percentage organic matter was calculated from the measured total organic carbon value.

We used the 129 sample K values and a kriging interpolation method to distribute spatially the soil erodibility factor (grid section of Arc-Info software). The whole basin was characterized by a single R_b value equal to 30 (t m mm ha^{-1} h^{-1}) estimated by the Sicilian isoerosivity map [*Ferro et al.*, 1991]. We used a crop factor C_b equal to 0.45 and a thickness of the cultivation layer Z (meters) equal to 0.1 because Sparacia basin, excluding a little undisturbed area located in its upper part, has been used exclusively for wheat cropping. Since management works are not carried out in the experimental basin, the support practice factor P was assumed to be equal to 1.

According to *Walling and Quine* [1990] the ^{137}Cs technique can be used to study the mobilization of sediments by erosion and the movement of sediments through the delivery system over the past 30 years by measuring the spatial distribution of ^{137}Cs. The ^{137}Cs technique is now well documented [*Ritchie et al.*, 1974; *Walling and Bradley*, 1988; *Ritchie and McHenry*, 1990; *Walling and Quine*, 1991; *Owens et al.*, 1997], and its review is beyond the aim of this paper.

The ^{137}Cs technique is based on the following key assumptions: (1) uniform local fallout distribution, (2) rapid adsorption of cesium 137 fallout onto soil particles, (3) subsequent redistribution of cesium 137 due entirely to sediment movement, and (4) ability to derive estimates of rates of soil loss from inventories of soil cesium 137. Measurement of ^{137}Cs input is commonly carried out at undisturbed sites where no erosion or deposition has occurred and the original fallout activity Cs_{ref} still remains. Where soil erosion has occurred, ^{137}Cs will have been lost, and ^{137}Cs is less than Cs_{ref}. Conversely, where soil deposition has taken place, an increase in ^{137}Cs activity will be found.

For relating ^{137}Cs losses to rates of soil erosion and deposition the simple proportional method of *Martz and de Jong* [1987] is widely applied. The proportional method assumes that depth of soil lost is directly proportional to ^{137}Cs lost. According to *Martz and de Jong* [1987, p. 422], "If soil tagged with ^{137}Cs is lost from the surface by erosion, untagged soil will be incorporated into the cultivation layer from below by tillage. As a result, the cultivated layer is maintained at a constant thickness while its ^{137}Cs content declines."

Using point measurement of soil cesium 137, Cs_i, the corresponding net soil loss E_i (kg m^{-2}) is calculated by the following equation [*de Jong et al.*, 1983]:

$$E_i = \frac{BD\ Z}{N} \frac{(Cs_{ref} - Cs_i)}{Cs_i} \quad (37)$$

in which BD is the bulk density [kg m^{-3}] and N is the number of years since atmospheric fallout of ^{137}Cs. For studying its spatial variability, the random variable ^{137}Cs activity [mBq cm^{-2}] was considered a regionalized variable, i.e., a variable developing in space and possessing a certain structure. The cesium 137 spatial distribution was obtained by a kriging interpolation method [*De Marsiliy*, 1986; *Ferro et al.*, 1998b] by GRID section of ARC-INFO software. A discretized map of the basin is obtained dividing the basin into morphological units and stream tubes, aggregating morphological units to define a concave hydraulic path. We overlayed the polygons of the discretized map and the raster cover of ^{137}Cs spatial distribution and then calculated net soil loss E_i in kilograms for each morphological unit or stream tube by (37), taking into

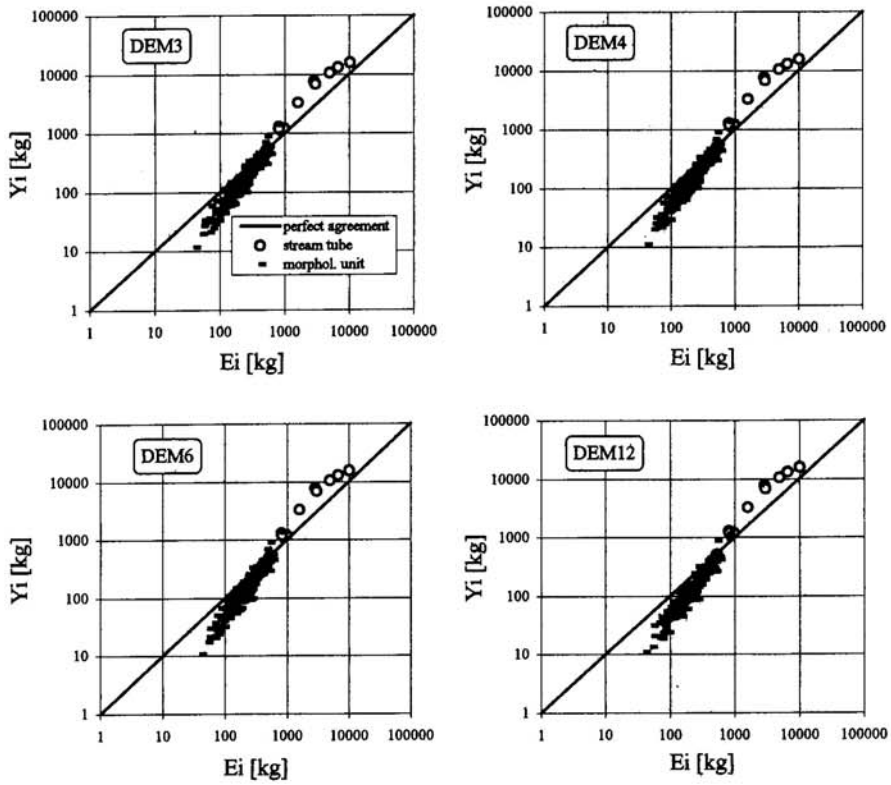

Figure 7. Comparison between measured net soil loss and calculated sediment yield at stream tube and morphological unit scale (RUSLE model).

account all square cells that fall into the polygons (morphological unit or stream tube).

To calculate the topographic factor of each morphological unit, slope has to be evaluated. Digital elevation models of the basin were derived from mesh sizes of 3, 4, 6, 8, and 12 m. The spatial distribution of slope is a raster cover of given mesh size. This is overlayed on the basin discretization map to calculate the slope s_i of each i morphological unit. For each polygon, s_i is the weighted mean, with weight equal to the area, of the slope values that fall within a polygon.

4.2. Experimental Results

To test the reliability of (22) and (35) coupled with (9) and (10), we compared the measured net soil loss E_i (kilograms) and the computed sediment yield Y_i, selecting an expression for topographic factor. The comparison was first carried out at morphological unit or stream tube scale (Figure 7). Figure 7 shows that the agreement between measured E_i and calculated Y_i values is independent of mesh size (ms) and that the calculated sediment yield values were generally lower than the measured values at the morphological unit scale but overstated at the stream tube scale.

We also carried out a comparison at the basin or subbasin scale. The sediment production at the basin or subbasin outlet Y_b was calculated by summing the sediment from all morphological units or stream tubes. In the same way the net soil loss at the basin or subbasin outlet E_b was calculated by the measured E_i values. For example, Figure 8 (ms = 4) shows a good agreement between Y_b and E_b even though the model tended to underestimate the smallest E_b values ($E_b < 21{,}000$ kg) and to overestimate the largest ones.

For calculating the slope exponent m, *McCool et al.* [1987] suggested the following expression:

$$m = \frac{af}{1 + af} \tag{38}$$

in which a is a numerical constant and f has the following expression:

$$f = \frac{\sin \alpha}{0.0896(3 \sin^{0.8} \alpha + 0.56)}. \tag{39}$$

According to *McCool et al.* [1987], f is the ratio of rill to interrill erosion, and for $a = 1$ and $f = 1$, indicating that rill and interrill erosion are equal, the slope length exponent m is 0.5.

McCool et al. [1989] suggested that for conditions where rill erosion is slight with respect to interrill erosion a coefficient a of (38) equal to 0.5 has to be used. A coefficient $a = 2$ corresponds to conditions where rill erosion is greater than interrill erosion.

Recently, *Di Stefano et al.* [1998], using cesium 137 measurements available for the Sicilian Sparacia basin [*Ferro et al.*, 1998b] for the Australian Hunter Valley basin [*Morris and Loughran*, 1994] and sediment yield measurements carried out at event scale in three experimental Calabrian basins [*Callegari et al.*, 1994; *Cantore et al.*, 1994; *Cinnirella et al.*, 1998], deduced the following relationships linking the constant a (Figure 14a) and the slope exponent p with the ms:

$$a = 0.2387 - 0.0070 \text{ ms} \tag{40}$$

$$p = 0.3483 - 0.0087 \text{ ms} \tag{41}$$

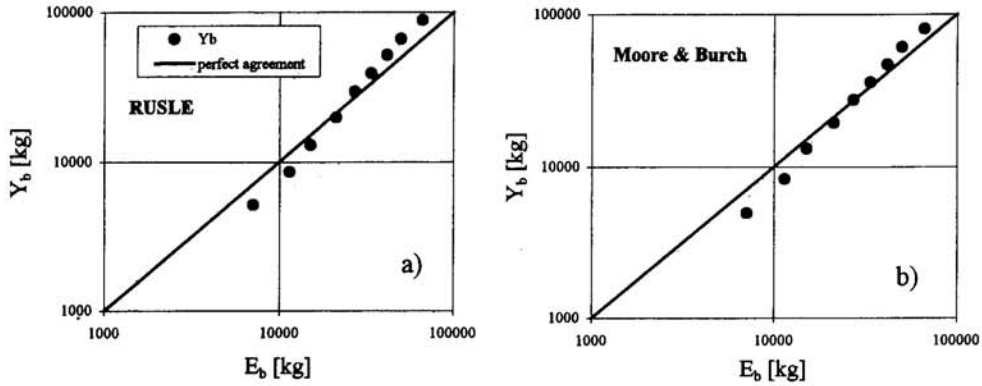

Figure 8. Comparison between measured net soil loss and calculated sediment yield at basin scale.

Figure 9 shows good agreement between measured net soil loss E_i and computed sediment yield values and confirms that the agreement is independent of mesh size. The comparison between Figures 7 and 9 shows that the underestimate and overestimate problems were solved using (40).

By using (40) and (41) for calculating the slope exponents (m and p), a good agreement between Y_b and E_b was obtained (Figure 10). The agreement shown in Figure 10, as an example for the digital elevation model (DEM) having a ms equal to 4 m, is also better than that plotted in Figure 8. In conclusion, the analysis shows that the distributed approach to sediment delivery processes coupled with RUSLE, in which a correction factor of the topographic factors for concave slopes and a new criterion for estimating the slope exponent of the topographic factors were introduced, has a good predictive ability at the morphological unit, in the stream tube, and at basin scales.

5. Conclusions

This research established that areas of severe erosion do not necessarily contribute the most sediment. Variation in transport capacity of different parts of a basin can change the picture. Therefore an analytical framework for estimating soil

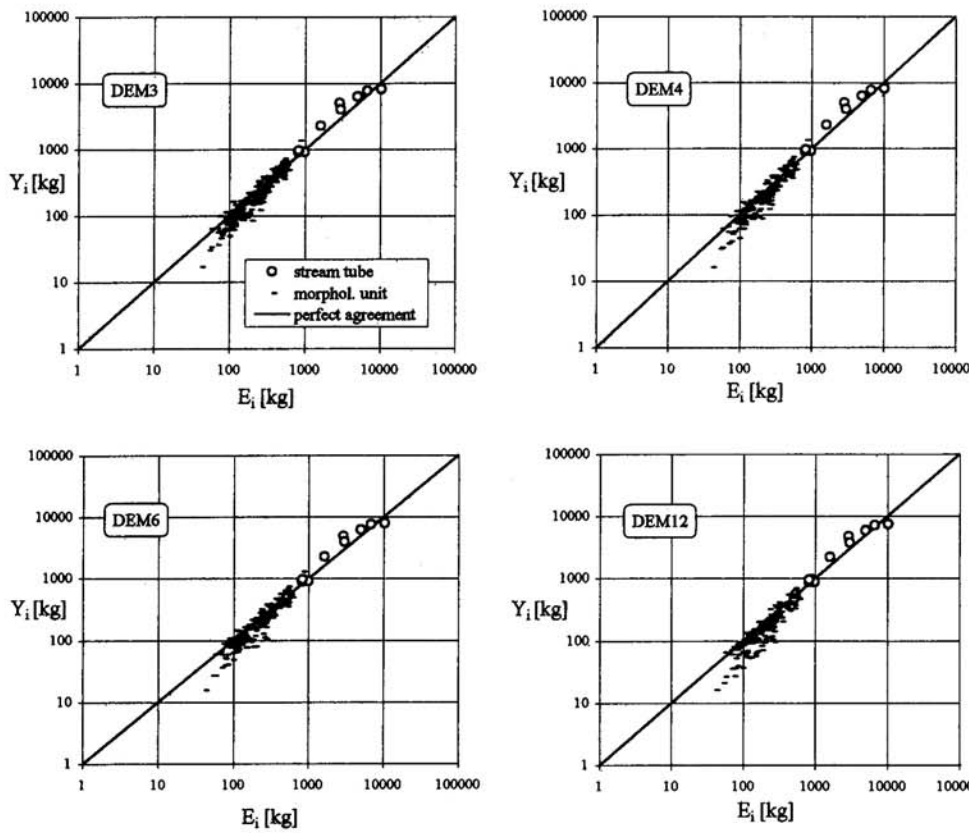

Figure 9. Comparison between measured net soil loss and calculated sediment yield for RUSLE model taking (40) into account.

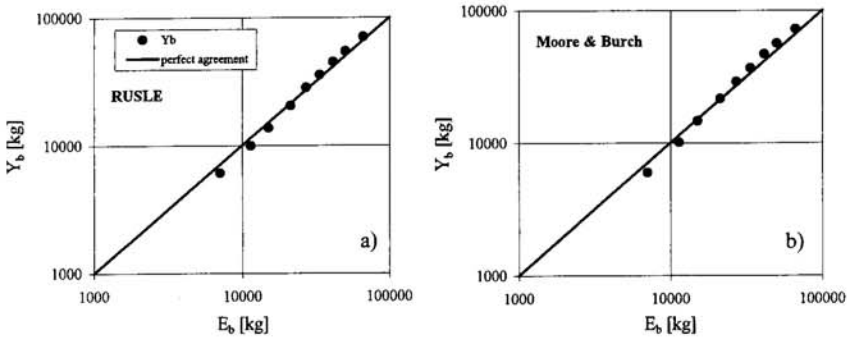

Figure 10. Comparison between measured net soil loss and calculated sediment yield at basin scale taking (40) and (41) into account.

loss and redistribution within a basin is needed to identify areas where soil conservation strategies will be effective for reducing sediment yield.

For estimating the basin sediment yield, i.e., the quantity of sediment which is transferred, in a given time interval, from eroding sources through the hillslopes and the channel network to the basin outlet, a plot-based soil erosion model can be coupled with a distributed mathematical operator expressing the sediment transport efficiency. In this paper, following a Lagrangian scheme, we modeled the sediment delivery processes along the hydraulic path from sediment source area to the nearest stream reach, accounting separately for the shape of the hydraulic path.

We have proposed describing a topographically complex landscape with a power equation (equation (5)), which allows for calculating the slope in each part of the profile. Then, using the RUSLE equation with two different expressions of the topographic factors, a criterion to define the erosion active profile, i.e., the slope length in which no deposition processes occur, is deduced.

For calculating the sediment load transported along the active slope length the continuity equation for sediment transport is integrated. In the solution of the integral equation having the same mathematical shape of RUSLE a Ψ factor is introduced for taking into account the influence of slope curvature in RUSLE. For testing the two topographic factor relationships (equations (22) and (35)) we used measured cesium 137 available from a Sicilian basin and the proportional method of *Martz and de Jong* [1987].

In particular, the comparison between calculated sediment yield Y_i and net soil erosion E_i values is carried out at morphological unit scale and by aggregating the morphological unit, which defines a concave hydraulic path (stream tube). Y_i values generally underestimated the measured E_i values at morphological unit scale, but Y_i overestimated E_i at stream tube scale. This result was also confirmed by a subsequent comparison at the basin or subbasin outlet. Finally, the underestimate and overestimate problems were solved by using appropriate slope exponents for the topographic factors, which vary with the mesh size of the DEM used to calculate the slope of each morphological unit into which the basin is divided.

In conclusion, the distributed approach to sediment delivery processes coupled with RUSLE, in which the topographic factors are corrected for taking into account the slope shape and a new criterion for calculating the slope exponent, is introduced. The results show a good predictive ability at different spatial scales (morphological unit, stream tube, and basin).

Acknowledgments. The research was supported by grants from Ministero Università e Ricerca Scientifica e Tecnologica (MURST), Governo Italiano, and Consiglio Nazionale delle Ricerche (CNR). V. Ferro and G. Tusa developed the mathematical model, and C. Di Stefano and P. Porto carried out the experimental validation. All authors set up the research, analyzed the results, and participated in writing the paper. C. Di Stefano developed this research for her Ph.D. activity, which is cofunded by the European Social Fund of the European Community. The authors acknowledge the reviewers who helped them to improve the final version of the manuscript.

References

Atkinson, E., Methods for assessing sediment delivery in river systems, *Hydrol. Sci. J.*, *40*, 273–280, 1995.

Bagarello, V., G. Baiamonte, V. Ferro, and G. Giordano, Evaluating the topographic factors for watershed soil erosion studies, in *Proceedings of the Workshop on Soil Erosion in Semi-Arid Mediterranean Areas*, edited by R. P. C. Morgan, pp. 3–17, Cons. Nazl. delle Ric., P. F. RAISA, Taormina, Italy, 1993.

Callegari, G., S. Cinnirella, and F. Iovino, Erosione e trasporto solido in piccoli bacini interessati da piantagioni di eucalitto, *Quad. Idronomia Mont.*, *13*, 139–150, 1994.

Cantore, V., F. Iovino, and S. Puglisi, Influenza della forma di governo sui deflussi liquidi e solidi in piantagioni di eucalitti, *Ital. For. Mont.*, *5*, 463–477, 1994.

Castro, C. D., and T. M. Zobeck, Evaluation of the topographic factor in the universal soil loss equation on irregular slopes, *J. Soil Water Conserv.*, *41*, 113–116, 1986.

Cinnirella, S., F. Iovino, P. Porto, and V. Ferro, Antierosive effectiveness of Eucalyptus coppices through the cover management factor estimate, *Hydrol. Proc.*, *12*, 635–649, 1998.

de Jong, E., C. B. M. Begg, and R. G. Kachanoski, Estimates of soil erosion and deposition for some Saskatchewan soils, *Can. J. Soil Sci.*, *63*, 607–617, 1983.

De Marsily, G., *Quantitative Hydrogeology: Groundwater Hydrology for Engineers*, Academic, San Diego, Calif., 1986.

Desmet, P. J. J., and G. Govers, A GIS procedure for automatically calculating the USLE LS factor on topographically complex landscape units, *J. Soil Water Conserv.*, *51*, 427–433, 1996.

Di Stefano, C., V. Ferro, and P. Porto, Comparing sediment yield and caesium-137 spatial distributions, paper presented at Conference on Agricultural Engineering, Ag Eng, Oslo, Norway, August 24–27, 1998.

Ferro, V., Further remarks on a distributed approach to sediment delivery, *Hydrol. Sci. J.*, *42*, 633–647, 1997.

Ferro, V., and M. Minacapilli, Sediment delivery processes at basin scale, *Hydrol. Sci. J.*, *40*, 703–717, 1995.

Ferro, V., G. Giordano, and M. Iovino, Isoerosivity and erosion risk map for Sicily, *Hydrol. Sci. J.*, *36*, 549–564, 1991.

Ferro, V., G. Giordano, and P. Porto, Validating a distributed approach of sediment delivery processes at basin scale, paper presented at XIII International CIGR Congress, Int. Comm. of Agric. Eng., Rabat, Morocco, February 2–6, 1998a.

Ferro, V., C. Di Stefano, G. Giordano, and S. Rizzo, Sediment delivery processes and the spatial distribution of caesium-137 in a small Sicilian basin, *Hydrol. Proc.*, *12*, 701–711, 1998b.

Foster, G. R., and W. H. Wischmeier, Evaluating irregular slopes for soil loss prediction, *Trans. ASAE*, *17*, 305–309, 1974.

Gradshteyn, I. S., and I. M. Ryzhik, *Table of Integrals, Series, and Products*, 5th ed., edited by A. Jeffrey, Univ. of Newcastle Upon Tyne, Newcastle, Engl., U. K., 1994.

Griffin, M. L., D. B. Beasley, J. J. Fletcher, and G. R. Foster, Estimating soil loss on topographically nonuniform field and farm units, *J. Soil Water Conserv.*, *43*, 326–331, 1988.

Julien, P., and M. Frenette, Scale effects in predicting soil erosion, *IAHS Publ.*, *159*, 253–259, 1986.

Julien, P., and M. Frenette, Macroscale analysis of upland erosion, *Hydrol. Sci. J.*, *32*, 347–358, 1987.

Kling, G. F., A computer model of diffuse sources of sediment and phosphorus moving into a lake, Ph.D. thesis, Cornell Univ., Ithaca, N. Y., 1974.

Martz, L. W., and E. de Jong, Using caesium-137 to assess the variability of net soil erosion and its association with topography in a Canadian prairie province, *Catena*, *14*, 439–451, 1987.

McCool, D. K., L. C. Brown, G. R. Foster, C. K. Mutchler, and L. D. Meyer, Revised slope steepness factor for the universal soil loss equation, *Trans. ASAE*, *30*, 1387–1396, 1987.

McCool, D. K., G. R. Foster, C. K. Mutchler, and L. D. Meyer, Revised slope length factor for the universal soil loss equation, *Trans. ASAE*, *32*, 1571–1576, 1989.

Meyer, L. D., and L. A. Kramer, Erosion equations predict land slope development, *Agric. Eng.*, *50*, 522–523, 1969.

Moore, I. D., and F. J. Burch, Physical basis of the length-slope factor in the universal soil loss equation, *Soil Sci. Soc. Am. J.*, *50*, 1294–1298, 1986.

Moore, I. D., and J. P. Wilson, Length-slope factors for the revised universal soil loss equation: Simplified method of estimation, *J. Soil Water Conserv.*, *47*, 423–428, 1992.

Morris, C. D., and R. J. Loughran, Distribution of caesium-137 in soil across a hillslope hollow, *Hydrol. Proc.*, *8*, 531–541, 1994.

Nearing, M. A., G. R. Foster, L. J. Lane, and S. C. Finkner, A process-based soil erosion model for USDA-Water Erosion Prediction Project Technology, *Trans. ASAE*, *32*, 1587–1593, 1989.

Novotny, V., and G. Chesters, Delivery of sediment and pollutants from nonpoint sources: A water quality perspective, *J. Soil Water Conserv.*, *44*, 568–576, 1989.

Onstad, C. A., C. L. Larson, L. F. Hermsmeier, and R. A. Young, A method of computing soil movement throughout a field, *Trans. ASAE*, *10*, 742–745, 1967.

Owens, P. N., D. E. Walling, Q. He, and J. Shanahan, The use of caesium-137 measurements to establish a sediment budget for the Start catchment, Devon, UK, *Hydrol. Sci. J.*, *42*, 405–423, 1997.

Renard, K. G., G. R. Foster, D. C. Yoder, and D. K. McCool, Rusle revisited: Status, questions, answers, and the future, *J. Soil Water Conserv.*, *49*, 213–220, 1994.

Richards, K., Sediment delivery and drainage network, in *Channel Network Hydrology*, edited by K. Beven and M. J. Kirkby, pp. 221–254, John Wiley, New York, 1993.

Risse, L. M., M. A. Nearing, A. Nicks, and J. M. Laflen, Error assessment in the universal soil loss equation, *Soil Sci. Soc. Am. J.*, *57*, 825–833, 1993.

Ritchie, J. C., and J. R. McHenry, Application of radioactive fallout caesium-137 for measuring soil erosion and sediment accumulation rates and patterns: A review, *J. Environ. Qual.*, *19*, 215–233, 1990.

Ritchie, J. C., J. A. Spraberry, and J. R. McHenry, Estimating soil erosion from redistribution of fallout ^{137}Cs, *Soil Sci. Soc. Am. J.*, *38*, 137–139, 1974.

Walling, D. E., The sediment delivery problem, *J. Hydrol.*, *65*, 209–237, 1983.

Walling, D. E., Erosion and sediment yield research-some recent perspectives, *J. Hydrol.*, *100*, 113–141, 1988.

Walling, D. E., and S. B. Bradley, The use of caesium-137 measurements to investigate sediment delivery from cultivated areas in Devon UK, in *Sediment Budgets*, edited by M. P. Bordas and D. E. Walling, pp. 325–335, Int. Assoc. of Hydrol. Sci., Gentbrugge, Belgium, 1988.

Walling, D. E., and T. A. Quine, Use of caesium-137 to investigate patterns and rates of soil erosion on arable fields, in *Soil Erosion on Agricultural Land*, edited by J. Boardman, I. D. L. Foster, and J. A. Dearing, pp. 33–53, John Wiley, New York, 1990.

Walling, D. E., and T. A. Quine, The use of ^{137}Cs measurements to investigate soil erosion on arable fields in the UK, potential applications and limitations, *Soil Science*, *42*, 147–165, 1991.

Wischmeier, W. H., and D. D. Smith, Predicting rainfall erosion losses from cropland east of the Rocky Mountains, *USDA Agric. Handb. 282*, U.S. Dep. of Agric., Washington, D. C., 1965.

Wischmeier, W. H., and D. D. Smith, Predicting rainfall erosion losses: A guide to conservation planning, *USDA Agric. Handb. 537*, U.S. Dep. of Agric., Washington, D. C., 1978.

Wischmeier, W. H., C. B. Johnson, and B. V. Cross, A soil erodibility nomograph for farmland and construction sites, *J. Soil Water Conserv.*, *26*, 189–193, 1971.

Young, R. A., and C. K. Mutchler, Effect of slope shape on erosion and runoff, *Trans. ASAE*, *12*, 231–239, 1969a.

Young, R. A., and C. K. Mutchler, Soil movement on irregular slopes, *Water Resour. Res.*, *5*, 1084–1089, 1969b.

C. Di Stefano, V. Ferro, P. Porto, and G. Tusa, Sezione Idraulica, Dipartimento di Ingegneria e Tecnologie Agro-Forestali, Università di Palermo, Viale delle Scienze, 90128 Palermo, Italy. (vferro@unipa.it)

(Received July 9, 1998; revised May 11, 1999;
accepted May 12, 1999.)